Computational analysis of the size effect in concrete fracture using gradient plasticity

Jian Chen, ALSTOM Power (Schweiz) AG, CH-5401 Baden, Switzerland
Huang Yuan, MTU Aero Engines GmbH, D-80995 Munich, Germany
Folker H. Wittmann, Aedificat Institute Freiburg, D-79104 Freiburg, Germany

Abstract

The size effect in cement-based composite materials, such as mortar and concrete, has been discussed for decades. It is known that the materials fracture energy increases with the specimen size, whereas the tensile strength decreases. It implies that the material strength measured on large specimens is not conservative for engineering applications. In this work we are using the gradient plasticity to investigate the size effect by means of the wedge splitting specimens. The computational simulations are controlled by the size-dependent fracture energy. It is shown that the intrinsic material length is correlated with the length of the fracture process zone linearly. Experiments can be reproduced using the gradient plasticity model for all specimens with 50 up to 3200 mm width. The computational predictions are independent of the finite element size due to the gradient regulator in constitutive equations. The results provide a uniform description to predict size-dependence of material strength.

Keywords: Size effect, concrete, gradient plasticity, finite element method.

1 Introduction

The size effect in cement-based materials has been discussed for several decades. The failure process of cement-based materials ranges from ductile to brittle with varying specimen sizes. According to Wittmann and co-workers [1, 2] the size effect is introduced due to interactions between the specimen boundaries and the fracture process zone. It has been confirmed that the fracture energy G_f [2] measured on small specimens, i.e. the uncracked ligament length of the specimen reaches the dimension of largest aggregates, significantly vary with the absolute specimen size. Should a specimen be large enough comparing to the aggregate size, the crack field is dominated by the property of the material around the tip. The resulting fracture energy for a driving crack is independent of the specimen size. If a characteristic size of the specimen approaches the dimension of aggregates, the fracture process zone becomes as large as the uncracked ligament. Crack initiation and propagation are strongly affected by specimen boundaries. It follows that the specimen failure depends on the specimen size. The crack resistance curve may significantly decrease with the specimen size as shown in [3].

In the present paper we continue the discussion of the size-dependent fracture energy initiated by Wittmann et al. [1, 2]. The investigation is based on computational analysis using the gradient plasticity combined with experimental records. Due to strain softening in the fracture process zone, the classical plasticity model cannot provide a unique prediction of the crack tip field. The gradient plasticity introduced by Aifantis [4] corrects this ill-conditioning in the governing equations, as reported by de Borst et al. [5, 6]. It has been shown that using the gradient plasticity model one may determine the shear band width or the damage zone size uniquely. The corresponding gradient coefficients turn out to relate directly to the internal length scales which characterize the underlying dominant microstructure.

The intention of the present paper is to use the gradient plasticity model to find out the materials intrinsic length in cementitous materials and to verify the size-dependent fracture energy concept. Computational simulations are validated by experimental results of wedge splitting tests on differently sized concrete specimens. Details of the experiments have been published earlier [2]. More detailed discussions about this simplification will be reported in a separate paper.

2 Computational models

2.1 Rankine plasticity model

Before we consider fracture process in the wedge splitting tests, a brief review of the gradient plasticity model is given in this section. More details about the model as well as the FEM implementation can be found in our previous publications [7] - [9].

The yield function of the modified Rankine plasticity can be written in the following form

$$F = \sigma_1 - \bar{\sigma}_g(\bar{\epsilon}^p, \nabla^2 \bar{\epsilon}^p), \quad (1)$$

where σ_1 denotes the maximum principal stress under plane stress condition. In the yield function we have assumed that the actual yield stress of the material depends on both equivalent plastic strain $\bar{\epsilon}^p$ and its gradient of the second order, $\nabla^2 \bar{\epsilon}^p$.

In the Rankine model the equivalent plastic strain rate, $\dot{\bar{\epsilon}}^p$, equals the amplitude of the first principal plastic strain rate $\dot{\epsilon}_1^p$, which is conjugate with the effective stress definition, that is,

$$\dot{\bar{\epsilon}}^p = |\dot{\epsilon}_1^p|. \quad (2)$$

If we adapt the associated plastic flow rule, the plastic strain rate can be evaluated as $\dot{\epsilon}^p = \dot{\lambda}\boldsymbol{n}$ with the plastic flow tensor $\boldsymbol{n} = \partial F / \partial \boldsymbol{\sigma}$, that is

$$\dot{\epsilon}_1^p = \dot{\lambda}. \quad (3)$$

The Rankine plasticity postulates that the material can plastically flow only if the maximum principal stress, σ_1, is positive. Consequently $\dot{\epsilon}_1^p$ has to be positive in the plastic zone and $\dot{\bar{\epsilon}} = \dot{\epsilon}_1^p = \dot{\lambda}$. It is clear that the Rankine yield surface for plane stress problems has a vertex peak in the principal stress plane, if the two principal stresses, σ_1 and σ_2, are positive. Pamin [6] suggested a modification to smooth the vertex yield surface, that is, when σ_1 and σ_2 are positive, the yield function (1) will be replaced by

$$F_s = (\sigma_x^2 + \sigma_y^2 + 2\sigma_{xy}^2)^{1/2} - \bar{\sigma_g}. \quad (4)$$

The corresponding equivalent plastic strain rate is re-defined as $\dot{\bar{\epsilon}}^p = \sqrt{\epsilon_x^2 + \epsilon_y^2 + \gamma_{xy}^2/2}$. It assures $\dot{\bar{\epsilon}}^p = \dot{\lambda}$.

Influence of Poisson's ratio in the analysis using the Rankine model is marginal. From the computational point of view, vanishing Poisson's ratio is advantageous to improve the robustness of the algorithm. This simplification makes the plane stress field equal to the plane strain field. For the brittle materials such a simplification will slightly effect the final prediction only.

2.2 Strain softening in a continuum

Bazant and Planas [10] pointed out that, if a continuum formulation based on stress-strain curves contains strain softening, it is necessary to complement it with some conditions that prevent the strain from localization into a region with zero dimension. Such conditions are generally called localization limiters. Aifantis [4] suggested that the actual yield stress in gradient plasticity theory can be assumed to be linearly dependent on both effective stress and strain gradient of the second order,

$$\bar{\sigma}_g(\bar{\epsilon}^p) = \bar{\sigma}(\bar{\epsilon}^p) - g\nabla^2 \bar{\epsilon}^p. \quad (5)$$

Consequently, the yield function can be expressed as follows

$$F = \Phi(\sigma) - \bar{\sigma}_g(\bar{\epsilon}^p, \nabla^2 \bar{\epsilon}^p) = 0. \quad (6)$$

In this equation the coefficient g is a function of the plastic strain, e.g.

$$g = -\bar{H}(\bar{\epsilon}^p) l^2, \quad (7)$$

where $\bar{H}$ is a dimensionless function and l has the length dimension. From the $1D$ shear band analysis with constant $\bar{H}$, de Borst and Mühlhaus [5] derived that the width of the shear band, h_c, and the intrinsic length l suggested by gradient plasticity have the relationship

$$h_c = 2\pi l. \quad (8)$$

Based on this analysis l is some kind of length scale of the material, for instance, shear band width. In more general cases identification of the parameter g is not a easy task. If g is constant, the yield function is dominated by the gradient term after over-proportional growth of $\nabla^2 \bar{\epsilon}^p$. It results in inconvergence of the computational iterations. In the large strain zone the strain gradient varies very strongly. From thermodynamics it follows that the gradient of the plastic strain should not dominate variations of the yield surface. Therefore, g should be a decreasing function of the plastic strain. For large strains and vanishingly small uniaxial yield stress $\bar{\sigma}(\bar{\epsilon}^p)$, g should approach zero. Otherwise, the material will not undergo damage. Based on such considerations we may assume

$$g = -\bar{\sigma}'(\bar{\epsilon}^p) l^2. \tag{9}$$

A similar form has been used by de Borst et al. [14] for cement-based materials, in which Equation (9) provides good agreement with experimental results.

Damage in the cement-based material will be modeled using the strain softening behaviour. The corresponding stress strain relationship is characterized by the fracture energy G_f. The varying G_f values change the local stress-strain relation. In the present work we use a single fracture energy value for a given specimen which is not consistent with the original concept of the size-dependent fracture energy for the inhomogeneous fracture process. The effect will be essential as the fracture zone spreads over the uncracked ligament. As a very first approach, however, we assume that such a simplification will not substantially affect our discussion. For our computations the Cornelissen-Hordijk-Reinhardt curve which was formulated originally in the context of cohesive cracking is adopted. The curve can be re-written in a continuum form [6] as

$$\begin{aligned} \bar{\sigma}(\bar{\epsilon}) &= f_t \left\{ \left[1 + \left(c_1 \frac{\bar{\epsilon}^p}{\bar{\epsilon}_u^p} \right) \right] \exp\left(-c_2 \frac{\bar{\epsilon}^p}{\bar{\epsilon}_u^p} \right) \right. \\ &\quad \left. - \frac{\bar{\epsilon}^p}{\bar{\epsilon}_u^p} \left(1 + c_1^3 \right) \exp(-c_2) \right\}, \end{aligned} \tag{10}$$

where $c_1 = 3.0$, $c_2 = 6.93$; f_t is the uniaxial

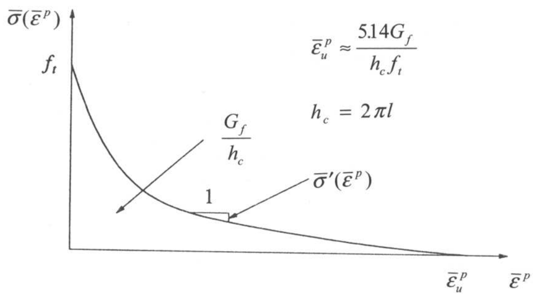

Figure 1: Nonlinear strain softening curve for cement-based materials under Mode I loading condition [15]. The stress is non-dimensionalized by yield stress.

tensile strength and $\bar{\epsilon}_u^p$ is the ultimate value of the equivalent fracture strain. The relation between the curve and the fracture energy G_f is assumed to be

$$\bar{\epsilon}_u^p = \frac{5.14 G_f}{h_c f_t}. \tag{11}$$

Variation of the yield strength is shown in Fig. 1 as a function of the plastic strain. Thus, the size-dependent fracture energy is related to the stress-strain correlation within the fracture zone.

The modified Rankine plasticity model with the strain gradient dependence has been implemented into the finite element code ABAQUS [11] using the user element interface. The implementation has been validated by extensive computational investigations [7, 8]. The gradient plasticity model has been further extended to nonlocal damage analysis for ductile materials [9]. For simplicity the finite element algorithms will not be repeated here. The readers are referred to our previous publications [8, 9] for more details.

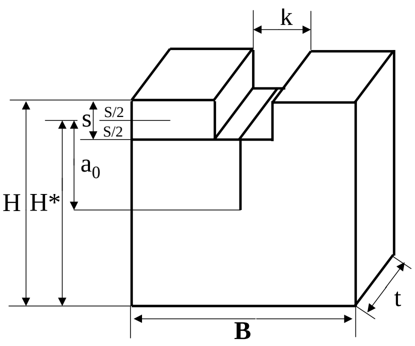

Figure 2: Geometry of the wedge splitting specimens.

3 Wedge splitting test and experimental results

Within the frame work of fracture mechanics research carried out at ETH Zurich a series of wedge splitting tests was performed and reported in [2]. The test set-up is similar to the one as described in RILEM recommendation AAC 13.1 (1994) [13]. The brittleness of concrete specimens and relatively low stiffness of the test machine makes it difficult to maintain a stable fracture process in a usual tensile test. The wedge splitting test overcomes these difficulties. Two wedges are pressed symmetrically between four roller bearings under controlled condition in order to split the specimen into two halves. The crack mouth opening displacement (CMOD) at both sides of the specimen at the level of the loading points, and the applied vertical load F can be measured [13]. From the measured vertical load and the known wedge angle the horizontal splitting force is calculated. All tests are run under CMOD control. The geo-

Table 1: Geometrical data of wedge splitting specimens studied in the present work

H mm	B mm	t mm	s mm	k mm	H^* mm	a_0 mm
100	100	200	30	40	85	42.5
200	200	200	30	40	185	92.5
400	400	400	100	100	350	175
800	800	400	100	100	750	375
1600	1600	400	100	100	1550	775
3200	3200	400	100	100	3150	1575

Table 2: Experimental results from wedge splitting tests

Height [mm]	100	200	400	800	1600	3200
F_{sp}^{max} [kN]	3.8	10.1	28.1	47.5	86.5	167.3
G_f^{exp} [N/m]	161	196	244	303	369	322
G_f^{num} [N/m]	156	188	251	297	387	340
f_t [N/mm^2]	2.43	3.36	2.42	2.10	1.95	2.5

metrical data are summarized in Table 1 based on the definitions as given in Fig. 2. The maximum aggregate size of the concrete is 32mm. The details of the experiment can be found in [2, 12, 13].

The fracture energy is evaluated based on the load vs. CMOD diagram [12]. In Table 2 we collect the fracture energy for crack initiation on the different sized specimens. It is obvious that the fracture energy G_f depends on the specimen size significantly. Based on our experimental data the fracture energy increases with the specimen size (Fig. 3). The stable value for the large specimen is more than twice as compared to the smallest specimen. Physically the size-dependence is related to the interaction of the fracture process zone with the boundaries of the specimens and with the aggregate size in the concrete, Φ_{max}.

To characterize the load vs. CMOD curves the maximum force f_t is the additional parameter except G_f. In the stress-strain relation the f_t describes the ultimate strength from the uniaxial tension. For the present work the f_t values have been computationally identified [2, 12, 13] based on experimental measurements. The results are shown in Fig. 4 and display that the maximum force is a decreasing function of the specimen size (Fig. 4), in which the force is normalized by the uncracked ligament area. Such variation can be explained based on the material defect distribution according to Weibull's weakest link theory which can be described by a power-law as

$$\frac{f_t}{f_{t0}} = \left(\frac{H}{H_0}\right)^m \tag{12}$$

with the Weibull parameter m=-0.093 as determined from experimental results.

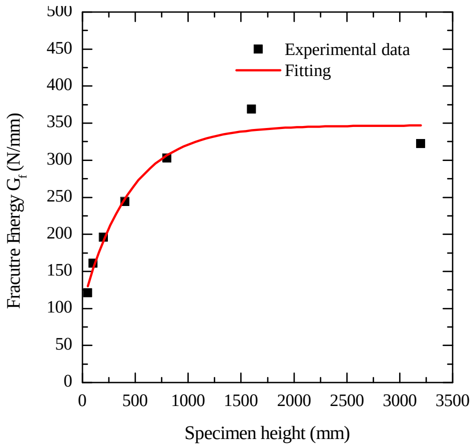

Figure 3: Size-dependent fracture energy from experimental results of the size effect [2, 13].

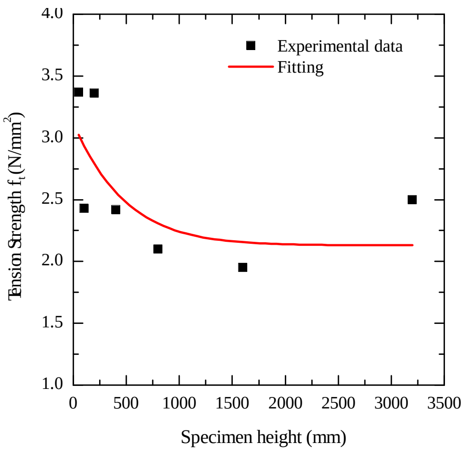

Figure 4: The tensile strength of the material determined from the wedge splitting tests from experimental results of the size effect [2, 13]

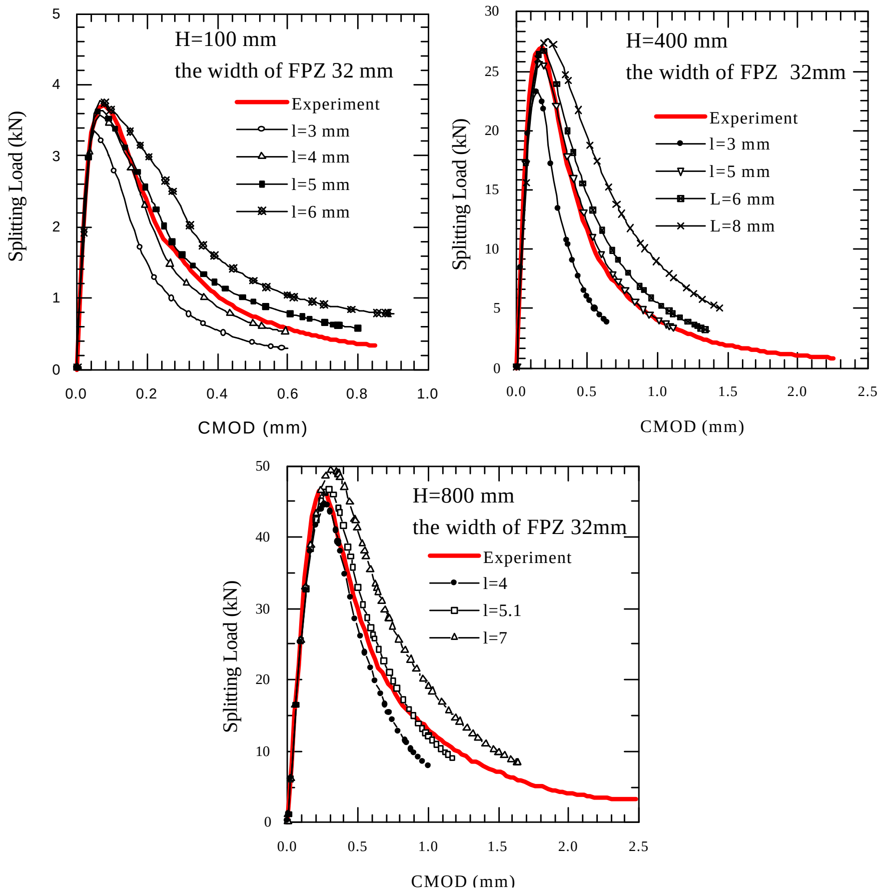

Figure 5: Influences of the intrinsic length l on the fracture energy and the tensile stress. The width of FPZ is assumed to be $h_c = 32$mm.

4 Computational results

4.1 Principles and assumptions

Gradient plasticity provides a unique prediction of crack propagation in concrete-like materials [5]. A key issue in the modeling is the identification of the material parameters, e.g. the strain-softening behaviour and the intrinsic material length. From the discussion of the fracture energy we expect that the strain-softening depends on specimen geometry and perhaps even the loading configuration. It means that the strain softening, which is related to the fracture energy, depends on the crack propagation. If the fracture process zone contacts the specimen boundary, the fracture energy and also the strain softening behavior become a function of the fracture process. It implies that the constitutive model for the material points near the specimen boundary has to take into consideration effects of the specimen boundary which makes the whole computation depended on the specimen geometry.

As the first approach we take the average fracture energy as our control value for the simulation, i.e. the fracture energy for each given specimen is unique. Such simplification will certainly effect the final results quantitatively, but not qualitatively. Here we are trying to figure out the internal correlation between the specimen geometry, aggregate size G_f, f_t and the material length parameter l. The final goal of this work is to verify the size-dependent fracture energy concept for concrete-like materials and to extend the fracture mechanics concept for structures with a small thickness comparing to the aggregate size.

In the computations using gradient plasticity we assume Young's modulus $E = 31500$ N/mm^2 and Poison ratio $\mu = 0.2$ for the elastic region. The values are confirmed with the previous experiments [2, 12, 13]. Effects of μ during material failure is negligible if the out-of-plane effect in the specimen will not be considered. The nonlinear strain softening curve is used for characterizing material damage. Due to the size-dependence in material failure it becomes necessary to implement the experimental results from the wedge splitting tests into our computational model. G_f and f_t are varying with the specimen sized as shown in Figs. 3 and 4. Note the values of G_f and f_t are fix for each given specimen, that is, they are independent of the failure process in each computation.

The computations are conducted under the assumption of the plane stress conditions. One half of the wedge splitting specimen is discretized using 8-nodal elements in the present computations. Using gradient plasticity makes the fracture process zone independent of the finite element size as reported in [6, 7]. The following discussions are concentrated on the evolution of the fracture process zone of differently sized specimens and its correlation with the intrinsic material length l or the parameter g in (5). To study effects of the specimen size on material failure we use the specimen-dependent fracture energy from experimental records to control computational simulations. Our computations practically give predictions of the specimen failure based on our fracture energy concept.

In 1D shear band analysis, de Borst and Mühlhaus [5] derived that the width of a shear band, h_c (8). For the normal concrete we may interpret the shear band as the damage zone. In multiaxial cases as on our specimens the relationship between the damage zone and the material length l is generally unknown. Hence we investigate the relationship between l and h_c by assuming different widths of the fracture process zone (FPZ) using the experimental results of the wedge splitting tests [13].

4.2 Correlation between the intrinsic length l and the aggregate size

In cement-based materials the fracture process zone is characterized by micro-crack initiation and coalescence, interface debonding between the aggregates and the hardened cement paste. As the very first approximation one simply uses a special stress-strain relationship for the fracture process zone and assume that the complex fracture process will be expressed by the strain softening.

The maximum aggregate size for our wedge splitting tests is $d = 32$mm [1, 2, 12]. The width of the fracture process zone (FPZ) can be assumed to be $h_c = 1d - 3d$. The specimen sizes considered in the present work vary between 50mm up to 3200mm. For the smallest specimens there is statistically only one aggregate in the uncracked ligament. The experimental records contain a large scatter. If we accept the assumption of the fracture process zone size, we see that the fracture process zone is even smaller than the uncracked ligament for H=100mm. For H=200mm the FPZ reaches the dimension of the uncracked ligament by $a_0/H = 0.5$. The fracture energy curve in Fig. 3 predict a size-dependent fracture process even up to H=750mm.

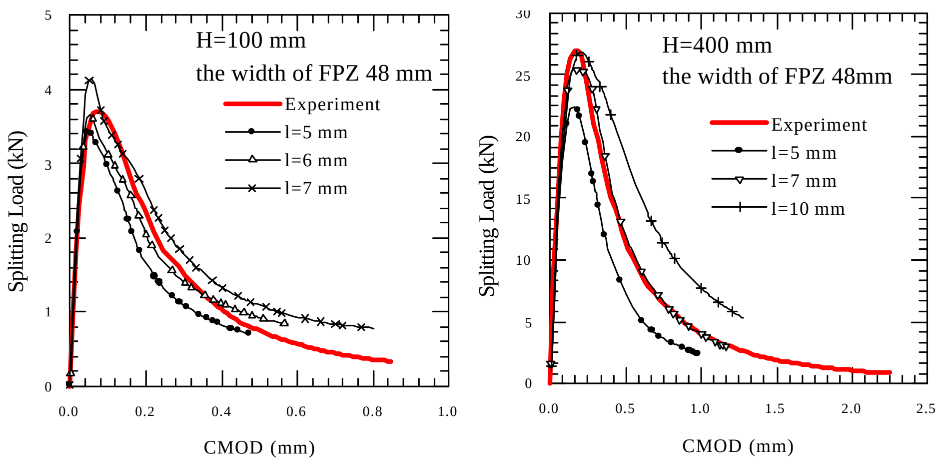

Figure 6: Influences of the intrinsic length l on the fracture energy and the tensile stress. The width of FPZ is assumed to be $h_c = 48$mm.

To investigate the correlation between the intrinsic material length l and the aggregate size, the computational crack propagation is controlled by the fracture energy curve in Fig. 3. The tensile strength f_t is taken from Fig. 4. The corresponding ultimate equivalent fracture strain $\bar{\epsilon}_u^p$ is derived from Equation (11). To identify the intrinsic material length, l is systematically changed for specimen H=100mm, 400mm and 800mm, respectively. Different widths of the FPZ, h_c = 32mm and h_c = 48mm, are assumed to investigate influence of the intrinsic length l. The corresponding fracture energy G_f and the tensile stress f_t are taken from Table 2. After assuming the value of the width of fracture process zone, h_c, the stress-strain curve defined by Equation (10) can be uniquely determined and used for numerical simulations.

The two series of computations are summarized in Figs. 5 and 6. In all computations increasing l leads to increase numerical material strength [8, 9]. For h_c = 32 mm we find that $l = 5$ mm provides the best fit for all three specimens. This confirms the validity of Equation (8) for the wedge splitting specimens. In Fig. 6 results are shown with h_c = 48 mm. Therefore, Equation (8) can be used for the nonlinear strain-softening analysis although it is derived from the linear strain-softening curve. The intrinsic length in gradient plasticity directly correlates with the width of the fracture process zone.

4.3 Prediction of failure in large specimens

Based on results reported in the last section we known that the gradient plasticity together with the size-dependent fracture energy enables us to reproduce experimental results. A main feature in the computational simulation is that the strain softening curve is controlled by the fracture energy. For specimens up to H = 800mm the fracture process is affected by the specimen size. Without corresponding correction the gradient plasticity model cannot predict the crack initiation and propagation in the concrete-like material.

For large specimens up to H =1600mm the fracture energy becomes size-independent (Fig. 3). It is interesting to know whether or not the gradient plasticity model can predict the material failure in large specimens, just based on a single strain-softening curve.

The width of the fracture process zone for normal concrete can be assumed to be 48mm

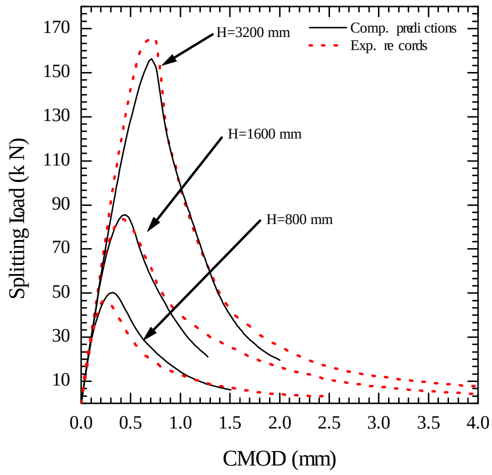

Figure 7: Numerical predictions of the mean load-deformation curves for all concrete specimens.

[12]. The numerical simulation has been carried out using the gradient plasticity model as for the specimen H = 800mm. The material parameters, $f_t = 2.5$ N/mm^2 and $G_f = 345$ N/m, are used for all specimens with different size ($H = 800 - 3200$ mm). To analyze the relation between the size effect and the material length, a unique stress-strain curve should be applied for all specimens. In Fig. 7 both numerical prediction and experimental records are summarized for quantitative comparison. Without additional tuning in material parameters we obtain excellent agreement between the experimental and computational results. The curves confirm that the gradient plasticity is suitable for failure modeling of concrete-like materials.

5 Discussions and conclusions

Both experimental and computational results confirm that the fracture process is affected by the specimen size as soon as the uncracked ligament approaches the dimension of the fracture process zone. If we do not want to change our conventional fracture mechanics concepts, we have to accept the size-dependent material parameters and, furthermore, to figure out the correlation between the parameters and the loading configuration.

The source of the constraint effects is the specimen boundaries. Under the small scale yielding conditions the crack tip field is well controlled by the leading crack parameter, as J-integral. If the inelastic zone in the metallic materials or the fracture process zone in the cement-based materials becomes so large that the second-order of the crack tip fields will be not negligible. It follows that the size effect is observed in experiments to determine fracture parameters. In this sense the fracture energy G_f contains both influences of material damage and the constraint effects and has to be a size-dependent material parameter. It will be interesting to find out the correlation between the stress distribution and the fracture energy value.

The strain-softening behaviour during material's failure is described by the gradient plasticity. The crack propagation is controlled by the size-dependent fracture energy as determined by corresponding experiments. From our computational analysis we may draw the following conclusions:

(1) Gradient plasticity provides an efficient model to simulate material damage using the strain softening curve. The numerical results agree with experimental records from differently sized specimens. The present computations confirm that the material damage process can be modeled using the strain softening curve combined with the size-dependent fracture energy criterion.

(2) The intrinsic material length l is uniquely correlated with the fracture process zone. We suggest to introduce the material length as an additional material parameter. To verify this point we need more extensive experimental and computational investigations for different aggregate size and different specimen geometries.

(3) The size-dependent fracture energy is caused by the interaction of the fracture process zone and the specimen boundaries. The gradient plasticity computations provide evidence of the size-dependent crack tip fields. It cannot be recommended to use the classical fracture mechanics concepts if the structural integrity of small sized specimens is to be predicted.

(4) The present study is limited to one type of specimens and one loading configuration. More extensive investigations are necessary to quantitatively validate the results.

References

[1] Duan, K., Hu, X.-Z. and Wittmann, F.H.. (2002). Explannation of size effect in concrete fracture using non-uniform energy distribution. *Materials and Structures*, **35**, pp. 326-331.

[2] Trunk, B. and Wittmann, F.H. (1998). Experimental investigation into the size dependence of fracture mechanics parameters. Proceedings FRAMCOS-2, pp. 79-88, Aedificatio Publishers, Freiburg, Germany.

[3] Carprinteri, A. (1994). Size-scale effects in the failure mechanics of materials and structures. *Proc. of Symp. on Size-Scale Effects in the Failure Mechanisms of Materials and Structures*, October 1994, Turin, Italy.

[4] Aifantis, E. C. (1987). The physics of plastic deformation. *International Journal of Plasticity*, **3**, pp. 211-247.

[5] de Borst, R., and Mühlhaus, H. (1992). Gradient-dependent plasticity:formulation and algorithmic aspects. *International Journal for numerical Methods in Engineering*, **35**, pp. 521-539.

[6] Pamin, J. (1994). Gradient-dependent plasticity in numerical simulation of localization phenomena. PhD Thesis, Delft University of Technology, Netherlands.

[7] Chen, J., and Yuan, H. (2002). A micromchanical damage model based on gradient plasticity: Algorithms and applications. *International Journal for Numerical Methods in Engineering*,**54**, pp. 399-420.

[8] Yuan, H., and Chen, J. (2001). Identification of intrinsic material length in gradient plasticity from micro-indentations. *International Journal of Solids and Structures*, **38** pp. 8171-8187.

[9] Chen,J., Yuan, H. and Wittmann, F.H. (2002). Computational simulations of micro-indentation tests using gradient plasticity theory. *Computer Modeling in Engineering and Sciences*, **6**, pp. 734-754.

[10] Bazant, Z.P. and Planas, J. (1997). Fracture an size effect in concrete and other quasibrittle materials. CRC Press, Boca Raton, FL, 1997.

[11] ABAQUS User Manual, Version 5.6, Hibbitt, Karlsson and Sorensen, Inc., Providence, R. I. (1996).

[12] Trunk, B. and Wittmann, F.H. (1998). Influence of size on fail of concarete. Proceedings FRAMCOS-3, pp. 1937-1948, Aedificatio Publishers, D-79104 Freiburg, Germany.

[13] Trunk, B. (2000). Einfluss der Bauteilgrsse auf die Bruchenergie von Beton. *ETH Laboratory for Building Materials, Building Material Report*, **No. 11**, Zurich, Switzerland.

[14] de Borst, R., Mühlhaus, H., Pamin, J. and Sluy, L.J. (1993). A continuum mechanics approach to concrte fracture. In *Numerical Models in Fracture Mechanics of Concrete*, ed. by F.H. Wittmann.

[15] Hordijk, D.A. (1991). Local approach to fatigue of concrete. *Dissertation, Delft University of Technology*, Delft, Nethderlands.